International Journal of Hydrogen Energy 250 (2026) 155980

Contents lists available at ScienceDirect

International Journal of Hydrogen Energy

journal homepage: www.elsevier.com/locate/he

Pressurized hydrogen from a liquid organic carrier – investigating the specific characteristics of hydrogen provision from 1,4-butanediol

J. Grüber [a], A. Seitz [a], L. Lami [a], S. Spahn [a], R. Stöber [b], T. Schärfe [a], F. Auer [a], M. Geißelbrecht [a,*], P. Wasserscheid [a,b,c,**]

[a] Forschungszentrum Jülich, Helmholtz-Institute Erlangen-Nürnberg for Renewable Energy (IET-2), Cauerstraße 1, Erlangen, 91058, Germany
[b] Forschungszentrum Jülich, Institute for a Sustainable Hydrogen Economy, Am Brainergy Park 4, Jülich, 52428, Germany
[c] Lehrstuhl für Chemische Reaktionstechnik, Friedrich-Alexander-Universität Erlangen-Nürnberg, Egerlandstr. 3, Erlangen, 91058, Germany

ARTICLE INFO

Keywords:
LOHC
1,4-Butanediol
Dehydrogenation
Copper
Dehydration

ABSTRACT

Liquid organic hydrogen carrier (LOHC) systems offer an attractive way to use the existing fuel infrastructure for the storage and transport of green energy equivalents. Traditional aromatic/alicyclic LOHC systems are fossil-based, use platinum metals, and require significant amounts of heat for hydrogen release. This contribution demonstrates technologically highly relevant features of the much less explored γ-butyrolactone (GBL)/1,4-butanediol (BDO) LOHC system. Our experiments show that the significantly lower dehydrogenation enthalpy of BDO (43.2 kJ mol_{H2}^{-1} compared to 68.3 kJ mol_{H2}^{-1} for, e.g., methylcyclohexane) enables robust, selective and highly productive hydrogen release under mild conditions. Hydrogen supply at elevated pressures from BDO is also possible and makes use of the high effective volumetric hydrogen storage density of BDO. Our data on catalyst stability, by-product formation, power density in hydrogen release, and purity of the released hydrogen in continuous BDO dehydrogenation further confirms the technical attractiveness of this previously largely overlooked LOHC system.

1. Introduction

The Liquid Organic Hydrogen Carrier (LOHC) technology offers an attractive way for the safe and energy-dense storage and transportation of hydrogen [1,2]. The technology relies on the catalytic binding of hydrogen through an exothermal hydrogenation reaction to the hydrogen-lean form of a given carrier system (H0-LOHC) producing its hydrogen-charged counterpart (Hx-LOHC). At the location and time of hydrogen or energy demand, the stored hydrogen can be released from the Hx-LOHC in an endothermal catalytic dehydrogenation reaction, whereby H0-LOHC is regenerated and can be used for a subsequent storage cycle.

While the endothermal nature of hydrogen release is a safety feature of all LOHC technologies (hydrogen release can be quickly stopped by interrupting the heat supply), it is fair to state that providing dehydrogenation heat at energy-lean times causes extra effort and energy investment if heat integration with waste heat sources is not possible. This makes LOHC systems with low enthalpies of hydrogenation/dehydrogenation particularly interesting because low enthalpy LOHC systems enable hydrogen release at milder conditions and lower heat investment. It has theoretically been demonstrated that LOHC systems with a hydrogenation/dehydrogenation enthalpy of around 40 kJ/mol H_2 result in particularly energy efficient and practical storage system [3]. At this value the reversibility of the hydrogenation/dehydrogenation sequence is fully ensured enabling effective charging and discharging of the LOHC system within technically attractive reaction conditions.

However, traditional aromatic/alicyclic LOHC systems (e.g. toluene/methylcyclohexane, or benzyltoluene (H0-BT)/perhydro benzyltoluene (H12-BT)) are characterized by hydrogenation/dehydrogenation enthalpies in the range of 65 to 70 kJ/mol H_2 (Table 1). Such enthalpies enable effective charging of the LOHC system at relatively modest hydrogen partial pressures (e.g. down to 10 bar [9]) but require high dehydrogenation temperatures (typically above 280 °C) for complete hydrogen release [10].

Historically, the first attempts to use low enthalpy LOHC systems

* Corresponding author.
** Corresponding author. Forschungszentrum Jülich, Helmholtz-Institute Erlangen-Nürnberg for Renewable Energy (IET-2), Cauerstraße 1, 91058, Erlangen, Germany
E-mail addresses: m.geisselbrecht@fz-juelich.de (M. Geißelbrecht), p.wasserscheid@fz-juelich.de (P. Wasserscheid).

https://doi.org/10.1016/j.ijhydene.2026.155980
Received 24 March 2026; Received in revised form 1 June 2026; Accepted 8 June 2026
Available online 18 June 2026

focussed on N-containing heteroaromatic/heteroalicyclic systems [11, 12]. However, a central promise of the LOHC concept is that the liquid carrier mixtures can use the existing infrastructure for liquid fuels and thus can facilitate an infrastructure-compatible and therefore faster transition to a fully defossilized energy system. In this context it is important to note, that the existing fuel system is not familiar with nitrogen-containing compounds and severe incompatibilities regarding tank, tube and sealing materials are obvious. This is different for oxygen-containing compounds: Biodiesel, methyl *tert*-butyl ether (MTBE), ethanol, and methanol are used or added to traditional fossil fuels up to large shares to improve their combustion properties or to limit their fossil CO_2 footprint. This makes all attempts to reduce the hydrogenation/dehydrogenation enthalpy of LOHC systems by the introduction of oxygen groups highly relevant.

Reported approaches include the acetone/isopropanol LOHC pair [13], the dehydrogenative esterification of ethylene glycol and ethanol to the ethyl-bridged diacetate ester (ethane-1,2-diyl diacetate) [14], and the reversible dehydrogenation of butanediol (BDO) to γ-butyrolactone (GBL). Hydrogen release from BDO has been described already in 2004 [15]. Later, in 2019, the complete storage/release cycle was reported using a homogenous Ir-based catalyst [16]. But only the thermodynamical assessment of Mevawala and coworker [8] and the use of Cu-based heterogeneous catalysts in repetitive BDO dehydrogenation/GBL hydrogenation (using pure hydrogen and syngas mixtures) cycles over many hundreds of hours in pressure-swing, batch mode operation [17] has more recently attracted a lot of attention to the GBL/BDO LOHC system for hydrogen storage, transportation and purification. Although the ethane-1,2-diyl diacetate/ethylene glycol/ethanol LOHC system exhibits highly favorable thermodynamic properties, currently reported hydrogenation and dehydrogenation studies using this system rely uniquely on the use of homogeneous catalysts [14]. In contrast, the GBL/BDO system has already demonstrated promising performance in heterogeneously catalyzed reactions enabling the study of continuous reactor operation with simple catalyst separation by solid separation [17].

Besides established petrochemical routes, BDO is accessible via biotechnological routes from biogenic raw materials [18] and neither BDO nor GBL is classified as a hazardous good for transportation. Most important is, however, that the required heat for hydrogen release is substantially lower for BDO dehydrogenation than for the dehydrogenation of N-heteroalicyclic or pure hydrocarbon alicyclic compounds (see Table 1). This opens the potential for integrating waste heat (e.g. from the energetic use of the released hydrogen) into the hydrogen release process [19]. The loading of GBL with hydrogen to produce BDO to close the LOHC cycle has been demonstrated as well [20]. This step works equally with Cu-catalysts and typical reaction conditions are 200 °C and 40 bar hydrogen pressure. Under these conditions selectivity is high, but conversion is not complete due to thermodynamics. This issue can be addressed by applying even higher pressures or by recycling the unreacted GBL after GBL/BDO separation.

This contribution focusses on BDO dehydrogenation. It compares the heat demand for the dehydrogenation of BDO with the respective values of methylcyclohexane and H12-BT dehydrogenation. Furthermore, the operational stability and by-product formation of continuous BDO dehydrogenation with a commercial Cu-based catalyst over extended time-on-stream is benchmarked against published data for the continuous dehydrogenation of H12-BT. We shed light on the hydrogen purity released from BDO and show that hydrogen release from BDO at elevated pressure can be carried out with little compromise on by-product formation. Because most technical hydrogen applications require hydrogen at elevated pressures, this unique feature of hydrogen provision from BDO safes the compression step or at least a large part of the required compression energy, depending on the pressure level of the targeted hydrogen use case.

2. Material and methods

2.1. Continuous dehydrogenation reactor

Continuous BDO dehydrogenation experiments were conducted in a vertical tubular reactor in upflow configuration with three electrically heated zones, an inner reactor diameter of 16 mm and a catalyst bed height of 400 mm. The resulting reaction volume amounted to around 80 mL. Six thermocouples were placed in 66.7 mm intervals along the reactor length, with the first and last positioned 33.3 mm from the top and bottom of the fixed bed, respectively. Additionally, two thermocouples were used to measure the temperature of the feed and product stream immediately before entering and after exiting the catalyst bed. The system pressure was controlled by a back pressure regulator (Equilibar). In the upstream section, BDO (Sigma-Aldrich, >99%) was dosed from a 12 L storage tank with a micro annular gear pump (HNP mzr-4605-hs-vb S/F) coupled with a Bronkhorst mini-Cori mass flow meter (MI130-tnn-33). Before entering the reactor, the BDO stream was preheated by flowing along a slit around a heating cartridge (Ø20 × 250 mm Türk + Hillinger). After the reactor, the products and unconverted reactants were condensed in a finned-tube coil heat exchanger. The resulting gas-liquid mixture was then separated in a coalescer (Boll & Kirch Filterbau). Liquid products were collected in condensate traps (Gustav Mankenberg Armaturenfabrik) before their cyclical removal to a product storage tank. The hydrogen stream was purified using an activated carbon filter cartridge (Contec GmbH) and quantified with a Bronkhorst mass flow meter. A schematic drawing of the experimental setup is depicted in Fig. 1.

The reactor was filled with 80.7 g of a commercially available CuO/ZnO/Al_2O_3 catalyst (HySat 430, Clariant) in tablet form (height 3-4 mm, diameter 5 mm). This catalyst material contains 39 wt% CuO and 39 wt % ZnO. The catalyst was reduced in situ at a set temperature of 175 °C using pure hydrogen at a flow rate of 0.1 L min^{-1} for 2.5 h in downflow operation mode. Due to the exothermicity of the reduction (caused by the formation of reaction water), the bed temperature increased above the setpoint, with average temperatures of 180–200 °C and transient hotspots reaching up to 300 °C. During the reduction, the temperature maximum moved from the top to the bottom of the reactor, indicating complete reduction after the 2.5 h reduction time (Supplementary Fig. 1).

Continuous H12-BT dehydrogenation was conducted in a

Table 1
Comparison of selected aromatic/alicyclic and O-containing LOHC systems with respect to their gravimetric and volumetric storage densities and their standard reaction enthalpy for hydrogen release from the respective Hx-LOHC compound. The reaction enthalpy of MCH and isopropanol are given for gas phase dehydrogenation. All other reactions are given as liquid phase reactions.

H0-LOHC	Hx-LOHC	H_2-capacity/wt.-%	H_2-capacity/Wh L^{-1}	$\Delta^rH_{Standard}$/kJ mol^{-1}	reference
Toluene (TOL)	Methylcyclohexane (MCH)	6.11	1567	68.3	[4]
Benzyltoluene (H0-BT)	Perhydro benzyltoluene (H12-BT)	6.18	1801	63.8	[5]
Dibenzyltoluene (H0-DBT)	Perhydro dibenzyltoluene (H18-DBT)	6.23	1888	65.3	[5]
Acetone	Isopropanol	3.33	864	55.5	[6]
Ethane-1,2-diyl diacetate	Ethylene glycol + ethanol	5.23	1562[a]	35.9	[7]
γ-Butyrolactone	1,4 Butanediol	4.44	1508	43.2	[8]

[a] An excess volume of 0 was assumed for calculating the density of the ethanol/ethylene glycol mixture.

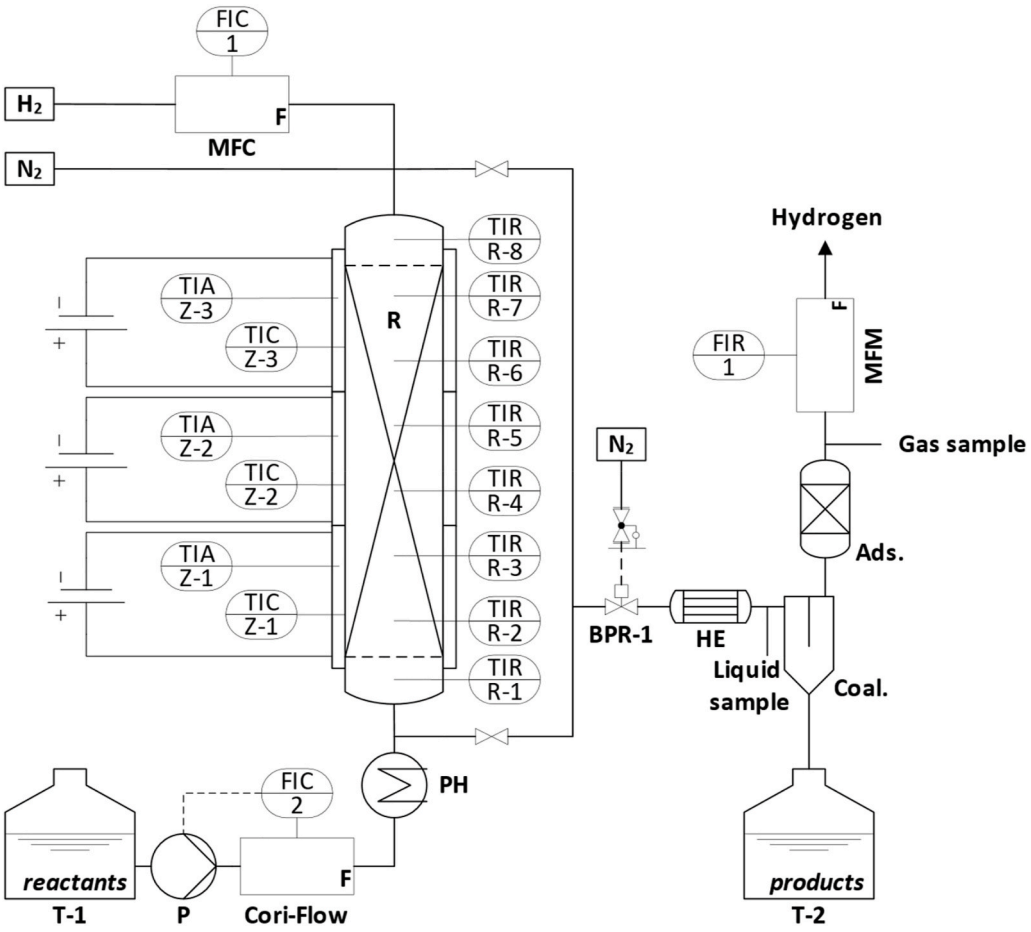

Fig. 1. Schematic process flow diagram of the applied BDO dehydrogenation setup with reactant tank (T-1), micro annular gear pump (P), reactant preheater (PH), reactor (R), heat exchanger (HE), coalescer (Coal.), activated carbon adsorber (Ads.) and product tank (T-2).

comparable setup as described by Willer et al. [21].

2.2. Semi-continuous BDO dehydrogenation at elevated hydrogen pressures

To evaluate the high-pressure dehydrogenation of BDO, a semi-continuous setup was used, with the liquid phase operated in batch mode and the gas phase released from the reactor in continuous mode. The setup comprised a 300 mL stainless-steel high-pressure/high-temperature autoclave (Parr Instruments, Type 4566). Temperature was controlled using an electric heating jacket and an internal cooling coil, both regulated by a Parr temperature controller (Type 4848). Reactor pressure was controlled using a Zero-Flow Series back pressure regulator (BPR) from Equilibar, which maintained a constant pressure during the reaction while released hydrogen was continuously removed. The hydrogen flow in the off-gas was quantified after condenser and BPR using a mass-flow meter (Bronkhorst, Type F–111B). Liquid samples were drawn regularly during the experiment.

High-pressure dehydrogenation was performed using the same Cu-based catalyst tablets (HySat 430, Clariant) as applied in the continuous experiments. Prior to reactor assembly, 6.095 g of the catalyst was placed in a catalyst basket inside the autoclave. Subsequently, the catalyst was reduced in situ at 200 °C and 2 bara under a continuous hydrogen flow of 0.9 L min^{-1} for 3 h. After reduction, the reactor temperature was set to 220 °C, the stirrer speed to 200 min^{-1}, and the control pressure of the BPR to 12 bara. To initiate the reaction, 200 g of BDO was introduced into the reactor via a liquid charging pipette using nitrogen pressure. In this setup, the gas-phase headspace was approximately 100 mL. At the operating pressure of 12 bara, this corresponded to an equivalent gas volume of about 1.2 L at normal conditions. At full conversion, 200 g of BDO release approximately 100 L of H_2 at normal conditions. We therefore assume that all nitrogen initially present in the autoclave is quickly purged from the reactor during the initial phases of the experiment.

2.3. Determination of performance indicators

Liquid products from continuous and semi-continuous dehydrogenation experiments were analyzed by gas chromatography (GC) using a Trace 1310 instrument (Thermo Fisher Scientific) equipped with an iConnect™ flame ionization detector (FID; Thermo Fisher Scientific) and an Rxi-17Sil capillary column (30 m × 0.25 mm i.d.; Restek). For GC-FID analysis, 30 µL of sample was diluted with 1 mL of acetone (Carl Roth GmbH, >99.9%). BDO, GBL, the intermediate products 2-hydroxytetrahydrofuran (2-HTHF) and 4-hydroxybutyl 4-hydroxybutanoate (4-HHB), and the side product tetrahydrofuran (THF) were separated, identified by comparison with commercial references and quantified using a GC-FID (Supplementary Fig. 2). Supplementary Fig. 3 illustrates the proposed reaction network including the intermediates 2-HTHF and 4-HHB, as well as the side-product THF formed via dehydration. Response factors F_i for BDO, GBL (Sigma-Aldrich, >99%), and THF (Sigma-Aldrich, >99.9%) were determined using commercially available standards (see Supplementary Table 1 in the ESI). The reference material for 2-HTHF and 4-HHB was only available commercially in limited quantities. These were suitable for identification but not for quantification. Therefore, their response factors were estimated based on the number of carbon atoms [22] (see Supplementary Table 1 in the ESI). An additional unidentified peak was observed and is hereafter

referred to as high boiler (HB; Supplementary Fig. 2). Because HB was found at a retention time similar to that of 4-HHB, it was assumed to have the same number of carbon atoms and was quantified using the response factor of 4-HHB (Supplementary Table 1). Other potential side products, such as dibutylene glycol and 1-butanol, were not detected in any of our experiments (Supplementary Fig. 2).

The response factors were used to convert the GC-FID peak areas A_i into corrected peak areas $A_{i,c}$ according to Equation (1):

$$A_{i,c} = \frac{A_i}{F_i} \tag{1}$$

Mole fractions were calculated from the corrected peak areas $A_{i,c}$ of all quantified compounds (BDO, GBL, 2-HTHF, 4-HHB, THF, HB) according to Equation (2).

$$x_i = \frac{A_{i,c}}{\sum A_{i,c}} \cdot 100\% \tag{2}$$

Hydrogen release from BDO was quantified by the degree of dehydrogenation (DoDH), defined as the ratio of the actual amount of H_2 released to the theoretical maximum H_2 releasable. DoDH was calculated from the mole fractions of the H_2-rich BDO, the H_2-lean GBL, and the partially loaded intermediate 2-HTHF (see Equation (3)). Because 4-HHB is formed via reversible dimerization of one BDO and one GBL [22], we treated this compound as an intermediate rather than as a side product causing LOHC material loss. Accordingly, 4-HHB was included into the DoDH calculation. THF and HB were considered side products (i.e., loss of cyclable LOHC material through dehydration) and were therefore excluded from the DoDH calculation. Note, that there might be ways to re-introduce dehydration side products into the original LOHC cycle by catalytic hydration or oxidation reactions (see below).

$$DoDH = \frac{2\frac{mol_{H2}}{mol_i}\left(x_{GBL} + 0.5\,x_{2-HTHF} + x_{4-HHB}\right)}{2\frac{mol_{H2}}{mol_i}\left(x_{BDO} + x_{GBL} + x_{2-HTHF} + 2\,x_{4-HHB}\right)} \cdot 100\% \tag{3}$$

The DoDH can also be estimated based on the released hydrogen flow detected via a mass flow meter $\dot{V}_{H2,\,N}$ and the BDO volume flow $\dot{V}_{BDO}$ according to Equation (4).

$$DoDH = \frac{\dot{n}_{H_2}}{\dot{n}_{H_2,max}} \cdot 100\% = \frac{\dot{V}_{H_2,N}}{2 \cdot \dot{V}_{BDO}} \cdot \frac{p_N \cdot M_{BDO}}{R \cdot T_N \cdot \rho_{BDO,20°C}} \cdot 100\% \tag{4}$$

$$with\ T_N = 273,15\ K, p_N = 1\ bar, R = 8,314\ J\ mol^{-1}K^{-1}, M_{BDO} = 90,12\ g\ mol^{-1}, \rho_{BDO,20°C} = 1,015\ g\ mL^{-1}$$

The gravimetric storage density of the hydrogen-rich LOHC molecule can be estimated using Equation (5), whereas $N_{H2,rev}$ is the number of reversibly storable hydrogen molecules and $M_{Hx\text{-}LOHC}$ is the molar mass of the hydrogen-rich LOHC molecule.

$$\rho_{mass} = \frac{2 \cdot N_{H2,rev}}{M_{Hx-LOHC}} \tag{5}$$

The volumetric storage density can be estimated using Equation (6), whereas $\rho_{Hx\text{-}LOHC}$ is the density of the hydrogen-rich LOHC molecule at ambient temperature and LHV_{H2} is the lower heat value of hydrogen.

$$\rho_{vol} = \rho_{mass} \cdot \rho_{Hx-LOHC} \cdot LHV_{H2} \tag{6}$$

The heat demand for the chemical reaction can be determined according to Equation (7) by multiplying the molar flow of released hydrogen $\dot{n}_{H2}$ with the reaction enthalpy $\Delta^r H$.

$$Q_{reaction} = \dot{n}_{H2} \cdot \Delta^r H \tag{7}$$

The amount of LOHC evaporation below the boiling temperature can be estimated by determining the vapor-liquid-equilibrium. If an activity coefficient of 1 and no hydrogen solubility in the liquid phase are assumed, the amount of evaporated LOHC is dependent on the molar flow of the released hydrogen $\dot{n}_{H2}$, the vapor pressure of the pseudo LOHC component $P^{LV}_{0,LOHC}$, and the total pressure. Equation (8) can be used to determine the amount of LOHC evaporation in the dehydrogenation and the LOHC losses after condensation.

$$\dot{n}_{evap} = \frac{\frac{P^{LV}_{0,LOHC}}{P}}{1 - \frac{P^{LV}_{0,LOHC}}{P}} \cdot \dot{n}_{H2} \tag{8}$$

The heat demand for LOHC evaporation in the dehydrogenation reactor can be estimated using Equation (9), whereas $\dot{n}_{evap}$ is the molar flow of evaporated LOHC and $\Delta^{g,l}H_{m,l}$ is the evaporation enthalpy.

$$Q_{evap} = \dot{n}_{evap} \cdot \Delta^{g,l} H_{m,H0-LOHC} \tag{9}$$

The sensible heat demand is according to Equation (10) dependent on the LOHC mass flow $\dot{m}_{LOHC}$, the heat capacity c_P and the temperature difference ΔT.

$$Q_{sens} = \dot{m}_{LOHC} \cdot c_P \cdot \Delta T \tag{10}$$

3. Results and discussion

3.1. Effective volumetric H_2 storage density and heat demand for H_2 release

Hydrogen storage capacity is a key parameter for comparing different LOHC systems. Most often such comparisons are carried out on a gravimetric basis. However, in many practical applications, volumetric rather than gravimetric storage density is the more relevant metric, as available space often represents the primary constraint in energy storage and logistics. Table 1 shows both values for selected LOHC systems. Focusing on the differences between MCH, H12-BT and BDO, it is noteworthy that the volumetric storage capacity between the pure hydrocarbon LOHC systems and BDO is considerably smaller than their difference in gravimetric capacity, owing to the substantially higher liquid density of BDO.

Moreover, the theoretical hydrogen storage capacity of an LOHC compound is rarely fully accessible in technically relevant systems. Not all chemically bound hydrogen can be released or utilized, because a certain fraction must be spent to supply the heat required for the endothermic dehydrogenation if no waste heat sources are available and integration of the waste heat from the energetic use of the released hydrogen is not possible. Therefore, a meaningful comparison of H12-BT, MCH and BDO for stand-alone or mobile applications requires balancing the heat demand of dehydrogenation to determine an effective volumetric hydrogen storage capacity.

For this comparison, a hydrogen release rate of 4.17 g s^{-1} was selected, corresponding to an energy output of 500 kW based on the lower heating value of hydrogen. For all three LOHC molecules under consideration, the dehydrogenation was assumed to reach a degree of dehydrogenation (DoDH) of 85% and the operating pressure was fixed at 5 bara. For H12-BT and MCH dehydrogenation, an isothermal catalyst temperature of 320 °C was assumed. Taking into account the lower reaction enthalpy of BDO dehydrogenation and the more favorable equilibrium at lower temperature resulting thereof [15,17], BDO dehydrogenation was assumed to take place at a catalyst temperature of 210 °C. All relevant thermophysical parameters for the following calculations are summarized in Table 2.

The heat demand for the dehydrogenation reaction can be estimated based on the amount of hydrogen released using the reaction enthalpy. For the selected hydrogen flow rate, the reaction heat demand is 139.4 kW for H12-BT, 146.0 kW for MCH, and only 90.0 kW for BDO dehydrogenation. These calculations for H12-BT and BDO dehydrogenation were all performed on the assumption that the reaction takes place entirely in the liquid phase. Since the evaporation enthalpies for H12-BT and H0-BT are very similar, the reaction enthalpy for the gas-phase reaction hardly changes compared to the liquid-phase reaction. Since the evaporation enthalpies of GBL is significantly lower than that

Table 2
Parameters for estimating the heat demand of H12-BT, MCH and BDO dehydrogenation. $\Delta^{r}H$ is the reaction enthalpy at reaction conditions, $\Delta^{g,l}H_m$ the evaporation enthalpy, P_0^{LV} the vapor pressure and c_p the specific heat capacity. All parameters for the H12-BT/H0-BT system are given at 320 °C. All parameters for the BDO/GBL system are given at 210 °C. All parameters with the exception of the evaporation enthalpy for MCH/TOL are given at 320 °C (evaporation enthalpy of this system is given at the normal boiling point).

Parameter	H12-BT	H0-BT	BDO	GBL	MCH	TOL
$\Delta^{r}H$/kJ mol_{H2}^{-1}	67.0 [5]		43.2 [8]		70.0	
$\Delta^{g,l}H_m$/kJ mol^{-1}	42.0 [23]	45.0 [23]	67.4 [24]	44.8 [25]	32.3 [26]	33.5 [26]
P_0^{LV}/bar	2.6 [27]	2.2 [27]	0.6 [28]	1.1 [28]	81.8 [29]	32.6 [29]
c_p/J g^{-1} K^{-1}	2.7 [5]	2.2 [5]	3.3 [30]	1.9 [31]	2.7 [32]	2.1 [32]

of BDO, the reaction enthalpy for the gas-phase dehydrogenation of BDO is reduced by the difference of the evaporation enthalpy of BDO and GBL. However, this effect is taken into account when calculating the enthalpy of evaporation.

The enthalpy required for LOHC evaporation depends on the fraction of the LOHC that evaporates inside the reactor. For H12-BT dehydrogenation, the H12-BT feed corresponds to 0.41 mol s^{-1}, and under the selected operating conditions, complete evaporation of Hx-BT is expected to occur within the reactor [33]. Accurate determination of the distribution between H0-BT and H12-BT evaporation would require a detailed reactor model. Here, we assumed an approximate evaporation of 50% H12-BT and 50% H0-BT on a molar basis. Based on this assumption, the resulting evaporation enthalpy for H12-BT dehydrogenation amounts to 17.8 kW. The vapor pressure of MCH is significantly higher than that of H12-BT. Consequently, MCH dehydrogenation is typically conducted with fully evaporated feed. MCH is evaporated in the preheating section of the reactor using the heat provided by TOL condensation downstream of the reactor. Therefore, no additional external heat input is required to cover the evaporation of MCH. Since BDO releases only two mols of hydrogen per mol of BDO, a feed flow rate of 1.22 mol s^{-1}- BDO is required to achieve the same hydrogen output. Using the approximation proposed by Kadar et al., an evaporation degree of 0.42 was estimated under the selected operating conditions [33]. To calculate the evaporation enthalpy, all evaporated species are considered as GBL. This assumption is made as the evaporation of BDO would reduce the reaction enthalpy by the difference in the evaporation enthalpy. This accounts for the fact that the evaporation of BDO followed by dehydrogenation requires the same amount of heat as the dehydrogenation of BDO followed by the evaporation of GBL. Based on this assumption, the resulting evaporation enthalpy for BDO dehydrogenation amounts to 23.0 kW.

During H12-BT and MCH dehydrogenation, complete evaporation occurs over a wide range of operating conditions, rendering the corresponding heat demand largely independent on process parameters. In contrast, for BDO, the evaporation enthalpy represents a substantially larger fraction of the total heat demand, and the degree of evaporation is strongly dependent on temperature and pressure. Consequently, suppressing complete evaporation by suitable operating conditions is essential to enhance the energetic efficiency of BDO dehydrogenation. The easiest way to avoid evaporation is to increase the reactor pressure, which has the additional benefit of supplying hydrogen at higher pressure to the downstream application. This may save significant investments in hydrogen compression, depending on the intended hydrogen application.

The heat demand for heating H12-BT and MCH after feed/product recuperation to the dehydrogenation temperature amounts to 2.1 kW (sensible heat). Please note, that we have assumed a temperature difference of 10 K between the temperature after recuperation and process temperature. The required sensible heat is slightly higher for BDO dehydrogenation (3.6 kW). However, in all cases the sensible heat contribution is an almost negligible part compared to the total heat demand.

For the estimation of the heat demand required for separating the LOHC material from the released hydrogen, it is assumed that the product flow is cooled to 30 °C in an air-cooled heat exchanger prior to gas–liquid separation. At this temperature, the vapor pressure of H0-BT is 1.2 Pa [23], resulting in an estimated LOHC material loss due to incomplete condensation of 1.5 10^{-3}%. This loss is considered negligible. Therefore, no additional cooling or compression is required, and no further heat demand arises from LOHC–hydrogen separation. In contrast, TOL exhibits a much higher vapor pressure of 4850 Pa at 30 °C [29], leading to an LOHC material loss of approximately 3.1%. This loss is unacceptably high, making additional cooling or compression necessary to limit LOHC material losses caused by incomplete condensation. For GBL, the vapor pressure at 30 °C is 71.5 Pa [28], corresponding to an LOHC material loss of 30.4 10^{-3}%. This loss is also regarded as acceptable, and therefore no additional heat input is assumed to be required for the GBL/hydrogen separation. Note, that for achieving comparable low LOHC losses in the TOL/hydrogen separation as for the GBL/hydrogen separation at 30 °C condensation temperature, the TOL–hydrogen product flow must be cooled to −37 °C. This additional cooling step would result in an additional heat demand of 8.6 kW.

If small amounts of LOHC impurities are inacceptable in the product hydrogen for the application in mind, hydrogen purification can be accomplished using temperature swing adsorption [34]. The associated heat demand is assumed to be comparable for all LOHC systems and is therefore not discussed further. The individual heat demand contributions for hydrogen provision from all three LOHC systems are summarized in Table 3.

Comparing the total heat demand for release (assuming a stand-alone or mobile scenario with no heat integration potential from the energetic use of the released hydrogen) with the LHV of the released hydrogen a stand-alone efficiency of hydrogen release can be calculated. The values are 0.68 for H12-BT dehydrogenation, 0.69 for MCH dehydrogenation, and 0.77 for BDO dehydrogenation. These results highlight the attractiveness of the BDO/GBL system, as significantly less heat is required for hydrogen release.

To further compare the three LOHC systems, the effective volumetric hydrogen capacity is introduced, which describes the amount of hydrogen that can be effectively utilized in a stand-alone hydrogen release unit without integrating heat or using external waste heat sources. Based on the calculated stand-alone efficiencies from above, the effective volumetric hydrogen capacity amounts to 1.04 kWh L^{-1} for H12-BT, 0.91 kWh L^{-1} for MCH and 0.98 kWh L^{-1} for BDO. Remarkably, these values are very close despite the substantial differences in gravimetric storage capacity between the pure hydrocarbon LOHC systems and the BDO/GBL system. This comparison also emphasizes that H12-BT has a significantly higher useable volumetric hydrogen capacity than MCH.

Another very important aspect that has not yet been taken into account in the numerical comparison above is that the dehydrogenation temperature in the case of BDO is about 100 °C lower than for the

Table 3
Comparison of the heat demand in the dehydrogenation of H12-BT, BDO and MCH to release 4.17 g s^{-1} of hydrogen (500 kW based on the LHV of the released hydrogen, DoDH of 85%, operating pressure of 5 bara).

Heat consumer	H12-BT	BDO	MCH
Reaction/kW	139.4	90.0	146.0
Evaporation/kW	17.8	23.0	-
Feed preheating/kW	2.1	3.6	2.1
Hydrogen purification/kW	-	-	8.6
Total heat demand/kW	**159.3**	**116.6**	**156.7**

dehydrogenation of MCH or H12-BT (due to the lower reaction enthalpy). Thus, heat integration with external heat sources is likely to be much easier due to the significantly lower temperature level of BDO dehydrogenation. For example, high-temperature proton exchange membrane fuel cells (HT-PEMFCs) can be operated at temperatures of up to 230 °C, which is suitable for heat integration with BDO dehydrogenation but not for heat supply to MCH or H12-BT dehydrogenation [4,20]. Such heat integration can increase in the case of BDO dehydrogenation the effective volumetric hydrogen capacity to 1.28 kWh L^{-1} (assuming still a ΔDoDH of only 85% during hydrogen release). Under such conditions, the effective volumetric hydrogen capacity of BDO would even exceed that of H12-BT (if heat integration for H12-BT is not possible due to its higher dehydrogenation temperature). These considerations demonstrate the very high attractiveness of the GBL/BDO LOHC system for technical hydrogen storage applications.

3.2. Catalyst stability, power density and by-product formation

To further evaluate the technical attractiveness of the GBL/BDO LOHC system, an assessment of the catalyst stability in BDO dehydrogenation is essential. High catalyst stability minimizes reactor downtime and cost associated with catalyst regeneration or replacement. Fig. 2 compares the operational stability of the established H12-BT dehydrogenation and the BDO dehydrogenation at a comparable DoDH. MCH is excluded from the following evaluations as its pure gas-solid reaction leads to relatively fast catalyst deactivation by coking that is countered in practical use cases by suitable catalyst regeneration measures.

For H12-BT dehydrogenation, the DoDH gradually decreases from an initial 80% to 65% over the first 24 h time on stream (TOS). After that stable performance is observed for the subsequent 15 h of operation. The observed deactivation is most likely caused by coke formation. Under the selected operating conditions, complete evaporation of Hx-BT occurs in some parts of the reactor. This makes effective removal of coke precursors via a liquid hot wash impossible for a certain part of the catalyst volume [35,36].

For BDO dehydrogenation, in contrast, an initial DoDH of approximately 75% was achieved under the applied conditions. This DoDH remained constant over 30 h TOS after which the experiment was terminated deliberately. Remarkably, even a slight increase in DODH was observed during the 30 h TOS which may be related to incomplete activation of the Cu-based catalyst at the start of the experiment. Note that an additional, independent BDO dehydrogenation experiment showed under the same conditions stable dehydrogenation performance over even 240 h TOS. These results indicate that coking is not a severe issue for BDO dehydrogenation under the conditions investigated. This is due to the different chemical nature of the LOHC system but also a consequence of the much milder conditions under which LOHC evaporation is minimized ensuring the continuous presence of liquid LOHC material within the reactor. This enables a constant hot-wash of all heavies from the catalyst surface preventing their accumulation and consecutive oligomerization reactions at the catalyst surface.

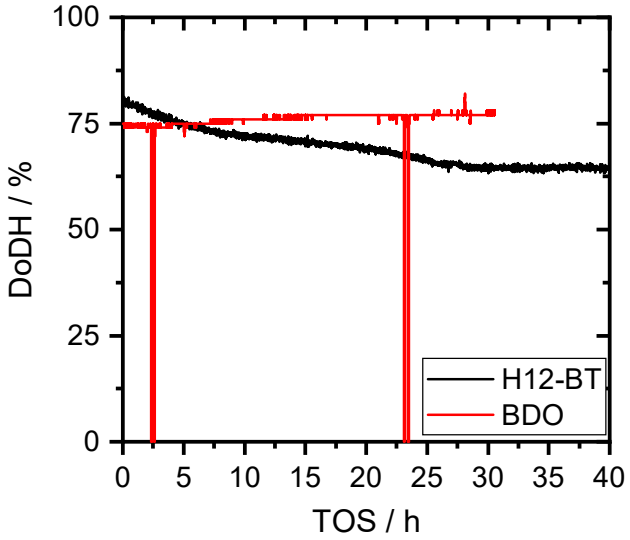

Fig. 2. Comparison of the catalyst and process stability for the dehydrogenation of H12-BT and BDO (the two sudden drops in the dehydrogenation of BDO are caused by sampling to determine the hydrogen purity). Conditions: H12-BT dehydrogenation: $T_{catalyst} = 315.8$ °C, p = 4 bara, 0.3 wt% Pt/Al_2O_3, $m_{catalyst} = 156.65$ g, $\dot{V}_{feed} = 5$ ml min^{-1}, $DoDH_{feed} = 2\%$; BDO dehydrogenation: $T_{catalyst} = 212.5$ °C, p = 4 bara, 39 wt% $CuO/ZnO/Al_2O_3$, $m_{catalyst} = 80.7$ g, $\dot{V}_{feed} = 2$ ml min^{-1}, $DoDH_{feed} = 0\%$.

Besides catalyst stability, power density of hydrogen release and the cyclability of the LOHC system are important criteria in the technological assessment of a LOHC system. High power density in the release step reduces the volume of the hydrogen release unit and paves the way for application in volume restricted applications, such as e.g. in heavy mobility applications. Cyclability is mainly governed by the amount and nature of by-product formation. In general, by-product formation should be kept to a minimum to preserve both the hydrogen storage capacity and the physico-chemical properties of the carrier molecule. Table 4 compares for continuous H12-BT and BDO dehydrogenation in steady-state operation these two relevant performance indicators at comparable DoDH and liquid hourly space velocity (LHSV).

The two operation points were selected to provide comparable space-time-yields (STYs) at similar DoDHs and LHSVs. Highly remarkably, this adjustment required to operate the BDO dehydrogenation at more than 100 °C below the temperature of H12-BT dehydrogenation. In other words, the same amount of hydrogen can be released from the same reactor volume using BDO and H12-BT dehydrogenation but at significantly milder conditions in the case of BDO dehydrogenation. High STY at low operating temperature is, therefore, identified as a quite unique feature of the GBL/BDO LOHC system and proven herein under steady-state continuous longterm operation. This unique feature is particularly valuable for mobile or decentralized applications where compact reactor design and efficient heat utilization are of utmost importance.

Our quantitative comparison of by-product formation focusses on the respective main by-products. These are methylfluorene (MF, a deep dehydrogenation product) in H12-BT [37] and tetrahydrofuran (THF, a dehydration product) in BDO dehydrogenation [15,17]. Furthermore, the sum of all high-boilers (i.e., all substances eluting later in gas chromatography than the main LOHC compounds) is compared. Under the investigated conditions and at the current state of catalyst and process development, higher by-product concentrations were observed for BDO dehydrogenation than for H12-BT dehydrogenation, namely 0.94 wt% THF and 0.32 wt% high boilers compared to 0.48 wt% MF and 0.11 wt% high boilers, respectively (see Table 4). Comparing the by-product formation of both LOHC systems, it has to be taken into account that BDO is technically more available and significantly less expensive than H12-BT. BDO can be produced from biogenic raw

Table 4
Comparison of the power density for H12-BT and BDO dehydrogenation. The results for the H12-BT dehydrogenation are given for the steady-state operation after 24 h TOS. Conditions: H12-BT dehydrogenation: p = 4 bara, 0.3 wt% Pt/Al_2O_3, $m_{catalyst} = 156.65$ g, $\dot{V}_{feed} = 5$ ml min^{-1}, $DoDH_{feed} = 2\%$. Conditions BDO dehydrogenation: p = 4 bara, 39 wt% $CuO/ZnO/Al_2O_3$, $m_{catalyst} = 80.7$ g, $\dot{V}_{feed} = 2$ ml min^{-1}, $DoDH_{feed} = 0\%$).

LOHC	$T_{catalyst}$/ °C	DoDH	LHSV/ h^{-1}	STY/kW L^{-1}	c_{MF}, c_{THF}/ wt.%	c_{HB}/ wt.-%
H12-BT	316.4	65%	1.68	1.57	0.48	0.11
BDO	212.5	75%	1.52	1.69	0.94	0.32

materials or polymer waste, which makes a regular refilling with fresh LOHC material less critical both from an economic and an ecological perspective [18,38].

3.3. High pressure hydrogen release from BDO

In many technical use cases, hydrogen is required at elevated pressure. Because the thermodynamic properties of the GBL/BDO LOHC pair enable dehydrogenation at elevated pressures [8], we were interested to verify whether such release of pressurized hydrogen is indeed viable with respect to achievable reaction rates and tolerable by-product formation. In contrast to conventional aromatic/alicyclic LOHC systems with comparatively high dehydrogenation enthalpies and large volume expansion (1 mol of H12-BT form 6 mol of hydrogen and 1 mol of H0-BT in full release), the significantly lower dehydrogenation enthalpy of the GBL/BDO system and the lower volume expansion in hydrogen release (1 mol of BDO forms 1 mol of GBL and 2 mol of hydrogen in full release) shifts the thermodynamic equilibrium less significantly towards the hydrogenated state at a given temperature when hydrogen partial pressures are increased. As a result, hydrogen release from BDO remains thermodynamically feasible even under elevated reactor pressures and comparatively mild temperature conditions, whereas such operation is thermodynamically strongly limited for aromatic/alicyclic LOHC systems. To the best of our knowledge, the direct production of hydrogen from an LOHC system at reactor pressures above 10 bar has not yet been reported in the literature. Besides saving compression energy, the operation of the BDO dehydrogenation at elevated pressures suppresses LOHC evaporation and with that the related additional heat demand. Furthermore, better heat transfer to the catalyst and better catalyst utilization can be achieved under conditions of reduced evaporation and enhanced liquid holdup. Fig. 3 shows the results of a semi-continuous dehydrogenation at 12 bara pressure and 220 °C reaction temperature. The hydrogen partial pressure in the reactor is 11.2 bar under the here applied conditions at the start of the reaction and decreases slightly due to the formation of the GBL reaction product.

Remarkably, a BDO conversion of nearly 90% was achieved at 220 °C in this semi-continuous dehydrogenation experiment demonstrating the feasibility of hydrogen release from BDO against elevated reactor pressure. The high-pressure conditions enhanced the undesired dehydration activity of the applied catalyst resulting in close to 10 mol% THF formation. THF formation represents a non-reversible side reaction within the primary BDO/GBL LOHC cycle. This side reaction results in loss of active LOHC material which reduces both cyclability and hydrogen yield, as hydrogen is consumed during the dehydration of BDO to THF.

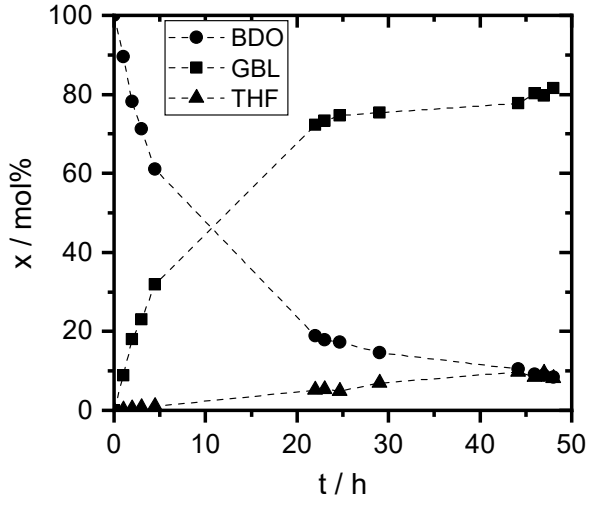

Fig. 3. Concentration profiles of the main reactants in the dehydrogenation of BDO against 12 bar total reactor pressure. Conditions: T = 220 °C, 39 wt% CuO/ZnO/Al_2O_3, $m_{catalyst}$ = 6.1 g, m_{BDO} = 200 g, $n_{stirrer}$ = 200 rpm.

Targeted catalyst optimization is now needed to suppress dehydration pathways at higher hydrogen partial pressures. Such developments are expected to fully unlock the potential of a direct provision of high-pressure hydrogen from BDO at comparatively mild temperature conditions. Note, that the formed THF side-product could be isolated by condensation from the hydrogen product stream. This isolated THF could be oxidized to GBL and other intermediates of the GBL/BDO cycle according to a literature report [39]. However, such regeneration step would have to take place outside the primary GBL/BDO cycle and would require additional process steps.

3.4. Hydrogen purity

Finally, we want to assess the purity of the hydrogen released from BDO under continuous steady-state dehydrogenation conditions. Hydrogen purity is a critical aspect for fueling low-temperature PEM fuel cells (LT-PEMFCs), but much less critical for fueling high-temperature PEM fuel cells (HT-PEMFCs), solid oxide fuel cells (SOFC), hydrogen combustion engines or hydrogen burners. Note, that if biogenic BDO is used the CO_2 in the exhaust gas of any oxidation process of impure hydrogen is also biogenic and does not contribute to the fossil CO_2 emissions. Herein, we determined the impurity concentrations in hydrogen released from BDO dehydrogenation and compare these data with results for H12-BT dehydrogenation from the literature as shown in Table 5 [34]. To ensure comparability, hydrogen purity was studied after condensation of organic vapor at 26 °C and after passing the gaseous product stream through an activated carbon adsorber in both cases. The BDO results originate from the dehydrogenation run displayed in Fig. 2.

While, hydrogen released from H12-BT under optimal conditions has been shown to meet the purity requirements for PEMFCs according to ISO 14687 [40], less favorable operation conditions and unpurified H12-BT can lead to much higher levels of impurities in H12-BT dehydrogenation. Hydrogen derived from BDO dehydrogenation exhibits – at the current state of catalyst and process development, and with the applied technical BDO quality - CO and CO_2 concentrations outside the limits specified in ISO 14687. However, the hydrogen released from BDO is already perfectly suitable for the operation of HT-PEMFCs [41–43]. Zilm et al. have reported that the hydrogen purity in H12-BT dehydrogenation is strongly dependent on the process conditions [34]. We therefore expect that optimizing the process conditions of BDO dehydrogenation and reducing the water content of the applied BDO (1500 ± 500 ppm) might also lead to improved hydrogen purity. Furthermore, catalyst optimization offers substantial potential to further suppress CO and CO_2 formation in BDO dehydrogenation.

4. Conclusion

In this study, technically highly relevant and new features of the

Table 5
Comparison of the impurities in the released hydrogen from continuous H12-BT and BDO dehydrogenation under steady-state conditions, respectively, after vapor condensation and active carbon adsorption. The data for H12-BT are taken from Ref. [34]. Conditions H12-BT dehydrogenation: T = 290-340 °C, p = 3-5.5 bara, 0.3 wt% Pt/Al_2O_3, $m_{catalyst}$ = 1400g, $\dot{V}_{feed}$ = 1-4.5 L h^{-1}, $DoDH_{feed}$ = 2%. Conditions BDO dehydrogenation: T = 210 °C, p = 4 bara, 30 wt% Cu CuZnAl, $m_{catalyst}$ = 80.7 g, $\dot{V}_{feed}$ = 2 ml min^{-1}, $DoDH_{feed}$ = 0%.

Entry	LOHC system	CO/ppm	CH_4/ppm	CO_2/ppm
1	H12-BT_{min}	0.09	18.2	0.34
3	H12-BT_{max}	13.10	36.7	1.72
3	H12-BT_{median}	2.58	22.7	0.48
4	BDO	3.50	n.d.[a]	1160

[a] Detection limit for methane is 1 ppm.

GBL/BDO LOHC system have been revealed in continuous, longterm BDO dehydrogenation experiments. Despite of BDO's modest gravimetric storage density of only 4.4%, the high liquid density of BDO (1.02 g/mL) leads to a comparable volumetric storage density compared to MCH. Taking the heat required for hydrogen release into account (assuming stand-alone hydrogen provision), the so-called effective volumetric hydrogen storage capacity can be calculated. Assuming a degree of dehydrogenation of 85% and operating pressure of 5 bara for a fair comparison of all three systems, this value is 0.97 kWh/L for hydrogen release from BDO compared to 1.04 kWh L^{-1} from H12-BT and 0.91 kWh L^{-1} from MCH, respectively. For application cases, in which waste heat is available (e.g. from the energetic use of the released hydrogen), the fact that the dehydrogenation temperature in the case of BDO is about 100 °C lower than for the dehydrogenation of MCH or H12-BT can open otherwise inaccessible ways of heat integration. This can make all hydrogen stored in BDO available for the respective application (up to 1.51 kWh L^{-1} based on the LHV of the released hydrogen).

Our study shows stable, continuous hydrogen release from BDO over a period of 30 h. This result suggests that coking, a typical deactivation mechanism for MCH or H12-BT dehydrogenation, is not a relevant problem for hydrogen release from BDO, at least under the conditions of the catalyst lifetime studies conducted here. The low formation of by-products and the high purity of the hydrogen released further underline the technical attractiveness of continuous hydrogen release from BDO. Our most important finding is, however, that BDO dehydrogenation enables the combination of high STY at low operating temperature (>100 °C lower than for H12-BT dehydrogenation with comparable productivity), which of utmost technical relevance for mobile or decentralized hydrogen supply scenarios.

Finally, we found in semi-continuous BDO dehydrogenation experiments that the GBL/BDO LOHC system enables hydrogen release at elevated pressure. We have shown that hydrogen release from BDO is possible at a hydrogen partial pressure of 11.2 bar and such process can make up to 80% of the BDO-stored hydrogen available under pressure. Although elevated reactor pressures enable the direct provision of compressed hydrogen and thereby reduce downstream compression demands, such operation requires a reactor design that can contain the targeted hydrogen pressure. More importantly, with the applied catalyst system, the increased hydrogen pressure leads to a higher level of undesired THF formation, resulting in reduced selectivity, lower hydrogen yield, and a loss of active LOHC material. Future catalyst optimization is required to suppress this dehydration pathways under high-pressure operating conditions. Despite the identified engineering challenges, we anticipate that BDO, pressure-less stored in conventional fuel tanks and released through Cu-based dehydrogenation at temperatures of 220 °C, can offer an attractive alternative for applications requiring moderate hydrogen pressures of up to approximately 11 bar, such as the supply of hydrogen to internal combustion engines or HT-PEMFC systems. The favorable operating conditions and the use of copper-based catalysts point to a very promising potential for the industrial scaling of the GBL/BDO LOHC system. However, further investigations into long-term stability, process integration and catalyst optimization, as well as detailed ecotoxicological and techno-economic assessments, are required to fully evaluate this potential for large-scale industrial application.

Declaration of generative AI and AI-assisted technologies in the manuscript preparation process

During the preparation of this work the authors used ChatGPT in order to edit the language. After using this tool/service, the authors reviewed and edited the content as needed and take full responsibility for the content of the published article.

CRediT authorship contribution statement

J. Grüber: Data curation, Investigation, Methodology, Validation, Writing – original draft. **A. Seitz:** Data curation, Methodology, Writing – original draft. **L. Lami:** Investigation, Methodology, Writing – original draft. **S. Spahn:** Investigation, Methodology, Writing – original draft. **R. Stöber:** Conceptualization, Data curation, Formal analysis, Methodology, Validation. **T. Schärfe:** Conceptualization, Data curation, Formal analysis, Methodology, Validation. **F. Auer:** Conceptualization, Data curation, Formal analysis, Methodology, Validation. **M. Geißelbrecht:** Conceptualization, Data curation, Formal analysis, Funding acquisition, Methodology, Supervision, Validation, Visualization, Writing – original draft. **P. Wasserscheid:** Conceptualization, Formal analysis, Funding acquisition, Methodology, Project administration, Resources, Writing – review & editing.

Conflict of interest

PW is co-founder and minority shareholder of Hydrogenious LOHC Technologies GmbH, Erlangen, a company that has commercialized equipment for hydrogen storage using the LOHC technology. There is no conflict of interest to declare with regard to the specific scientific results reported in this paper.

Acknowledgements

The authors acknowledge financial support by the Bavarian Ministry of Economic Affairs, Regional Development and Energy through the project “Oxo-LOHC - Autotherme und ultratiefe Wasserstofffreisetzung aus LOHC-Systemen” (84-6665a2/201/11). In addition, the authors gratefully acknowledge support by the Werner Siemens Foundation in the frame of the WSS Research Centre catalaix.

Appendix A. Supplementary data

Supplementary data to this article can be found online at https://doi.org/10.1016/j.ijhydene.2026.155980.

References

[1] Niermann M, Drünert S, Kaltschmitt M, Bonhoff K. Liquid organic hydrogen carriers (LOHCs)-techno-economic analysis of LOHCs in a defined process chain. Energy Environ Sci 2019;12:290–307. https://doi.org/10.1039/c8ee02700e.
[2] Aakko-Saksa PT, Cook C, Kiviaho J, Repo T. Liquid organic hydrogen carriers for transportation and storing of renewable energy–review and discussion. J Power Sources 2018;396:803–23. https://doi.org/10.1016/j.jpowsour.2018.04.011.
[3] Müller K, Völkl J, Arlt W. Thermodynamic evaluation of potential organic hydrogen carriers. Energy Technol 2013;1(1):20–4. https://doi.org/10.1002/ente.201200045.
[4] Schildhauer T, Newson E, Müller S. The equilibrium constant for the methylcyclohexane–toluene system. J Catal 2001;198(2):355–8.
[5] Müller K, Stark K, Emelyanenko VN, Varfolomeev MA, Zaitsau DH, Shoifet E, Schick C, Verevkin SP, Arlt W. Liquid organic hydrogen carriers: thermophysical and thermochemical studies of Benzyl- and dibenzyl-toluene derivatives. Ind Eng Chem Res 2015;54(32):7967–76. https://doi.org/10.1021/acs.iecr.5b01840.
[6] Haynes WM. CRC handbook of chemistry and physics. CRC press; 2016.
[7] Stein S, Brown R. Structures and properties group additivity model. In: NIST chemistry WebBook, vol. 69. NIST standard reference database; 2009, 20899.
[8] Mevawala C, Autrey T, Brooks K, Bowden M, Tran BL, Muller K. 1, 4-Butanediol as a hydrogen carrier: liquid-versus gas-phase dehydrogenation. Energy & Fuels 2022;37(1):560–6. https://doi.org/10.1021/acs.energyfuels.2c03355.
[9] Lippert J, Wasserscheid P, Geißelbrecht M. Continuous hydrogenation of the hydrogen storage compound benzyltoluene in a trickle-bed reactor–influence of mass transfer and optimization strategies. Int J Hydrogen Energy 2026;211:153617.
[10] Meda US, Raikar OM, Acharya A, Sg AK, Mahesh R, Shetty T. Nuances in liquid organic hydrogen carriers. Renew Sustain Energy Rev 2026;226:116237.
[11] Pez GP, Scott AR, Cooper AC, Cheng H. Hydrogen storage by reversible hydrogenation of pi-conjugated substrates. Google Patents; 2008.
[12] Sotoodeh F, Huber BJ, Smith KJ. The effect of the N atom on the dehydrogenation of heterocycles used for hydrogen storage. Appl Catal Gen 2012;419:67–72.
[13] Sievi G, Geburtig D, Skeledzic T, Bösmann A, Preuster P, Brummel O, Waidhas F, Montero MA, Khanipour P, Katsounaros I. Towards an efficient liquid organic hydrogen carrier fuel cell concept. Energy Environ Sci 2019;12(7):2305–14.

[14] Zhou QQ, Zou YQ, Ben-David Y, Milstein D. A reversible liquid-to-liquid organic hydrogen carrier system based on ethylene glycol and ethanol. Chem–Eur J 2020; 26(67):15487–90.
[15] Ichikawa N, Sato S, Takahashi R, Sodesawa T, Inui K. Dehydrogenative cyclization of 1, 4-butanediol over copper-based catalyst. J Mol Catal Chem 2004;212(1–2): 197–203.
[16] Onoda M, Nagano Y, Fujita K-i. Iridium-catalyzed dehydrogenative lactonization of 1, 4-butanediol and reversal hydrogenation: new hydrogen storage system using cheap organic resources. Int J Hydrogen Energy 2019;44(53):28514–20.
[17] Chen Y, Kong X, Yang C, Liao Y, Gao G, Ma R, Peng M, Shao W, Zheng H, Zhang H. A catalytic cycle that enables crude hydrogen separation, storage and transportation. Nat Energy 2025:1–10. https://doi.org/10.1038/s41560-025-01806-9.
[18] Burgard A, Burk MJ, Osterhout R, Van Dien S, Yim H. Development of a commercial scale process for production of 1, 4-butanediol from sugar. Curr Opin Biotechnol 2016;42:118–25.
[19] Wasserscheid P. Impurity-tolerant catalysis: liquid organic hydrogen carriers. Nat Energy 2025:1–2. https://doi.org/10.1038/s41560-025-01832-7.
[20] Ren X, Zhou M, Yu W, Zheng M, An Q. Catalytic hydrogenation of γ-Butyrolactone to butanediol over a high-performance Cu-SiO2 catalyst. Catalysts 2024;14(5):297.
[21] Willer M, Preuster P, Geißelbrecht M, Wasserscheid P. Continuous dehydrogenation of perhydro benzyltoluene and perhydro dibenzyltoluene in a packed bed vertical tubular reactor–the role of LOHC evaporation. Int J Hydrogen Energy 2024;57:1513–23. https://doi.org/10.1016/j.ijhydene.2024.01.031.
[22] Qasmi C, Mochel R, Gautier V, Champon I, Thomas S, Chappaz A, Anne-Cécile R. GBL/BDO pair as a bio-based liquid organic carrier: kinetic modeling of liquid phase hydrogenation and dehydrogenation over copper-based catalyst. Int J Hydrogen Energy 2024;67:829–41.
[23] Verevkin SP, Vostrikov SV, Leinweber A, Wasserscheid P, Müller K. Thermochemical properties of benzyltoluenes and their hydro-and perhydro-derivatives as key components of a liquid organic hydrogen carrier system. Fuel 2023;335:126618.
[24] Vasiltsova TV, Verevkin SP, Bich E, Heintz A, Bogel-Lukasik R, Domanska U. Thermodynamic properties of mixtures containing ionic liquids. Activity coefficients of ethers and alcohols in 1-methyl-3-ethyl-imidazolium bis (trifluoromethyl-sulfonyl) imide using the transpiration method. J Chem Eng Data 2005;50(1):142–8.
[25] Steele W, Chirico R, Nguyen A, Hossenlopp I, Smith N. Determination of some pure compound ideal-gas enthalpies of formation. Bartlesville, OK (United States …: National Energy Technology Lab.(NETL); 1989.
[26] Stephenson RM. Handbook of the thermodynamics of organic compounds. Springer Science & Business Media; 2012.
[27] Jorschick H, Geißelbrecht M, Eßl M, Preuster P, Bösmann A, Wasserscheid P. Benzyltoluene/dibenzyltoluene-based mixtures as suitable liquid organic hydrogen carrier systems for low temperature applications. Int J Hydrogen Energy 2020;45 (29):14897–906.
[28] Yaws CL. Thermophysical properties of chemicals and hydrocarbons. William Andrew; 2008.
[29] Brown RL, Stein SE. Boiling point data. 2001. Number.
[30] Petit JC, Ter Minassian L. Measurements of (∂ V∂ T) p,(∂ V∂ P) T, and (∂ H∂ T) p by flux calorimetry. J Chem Therm 1974;6(12):1139–52.
[31] Ismailov T, Gabzalilova N, Makhkamov KM. Complex study of physicochemical properties of γ-butyrolactone. Uzb Khim Zh 1988;4:48.
[32] Thermocenter G. Entropy and heat capacity of organic compounds. NIST chemistry WebBook, NIST standard reference database 2018;69.
[33] Kadar J, Gackstatter F, Ortner F, Wagner L, Willer M, Preuster P, Wasserscheid P, Geißelbrecht M. Boosting power density of hydrogen release from LOHC systems by an inverted fixed-bed reactor design. Int J Hydrogen Energy 2024;59:1376–87. https://doi.org/10.1016/j.ijhydene.2024.02.096.
[34] Zilm A, Ortner F, Gackstatter F, Koeberlein S, Kadar J, Geisselbrecht M, Boesmann A, Wasserscheid P. Impurities in hydrogen released from perhydro benzyltoluene-assessment and adsorptive removal. Int J Hydrogen Energy 2025; 101:469–81.
[35] Henseler J, Schärfe T, Steffen J, Görling A, Geißelbrecht M, Wasserscheid P. Detailed analysis of coke precursor formation in catalytic perhydro benzyltoluene dehydrogenation processes. Fuel 2025;398:135500.
[36] Guisnet M, Magnoux P. Organic chemistry of coke formation. Appl Catal Gen 2001; 212(1–2):83–96.
[37] Alconada K, Mariño F, Agirre I, Barrio VL. Exploring perhydro-benzyltoluene dehydrogenation using sulfur-doped PtMo/Al2O3 catalysts. Catalysts 2025;15(5): 485.
[38] Pang W, Li B, Wu Y, Zeng Q, Yang J, Zhang Y, Tian S. Upgraded recycling of biodegradable PBAT plastic: efficient hydrolysis and electrocatalytic conversion. Chem Eng J 2024;486:150342.
[39] Abduh NA, Al-Kahtani A, Algarni TS, Al-Odayni A-B. Selective oxidation of tetrahydrofuran to gamma-butyrolactone over spinel Znfe2o4 nanoparticle catalyst. Catalysts 2023;13(4):692.
[40] Standardization IOf. ISO/DIS 14687 hydrogen fuel quality–Product specification. Geneva, Switzerland: International Organisation for Standardization; 2019.
[41] Devrim Y, Albostan A, Devrim H. Experimental investigation of CO tolerance in high temperature PEM fuel cells. Int J Hydrogen Energy 2018;43(40):18672–81.
[42] Brouzgou A, Seretis A, Song S, Shen PK, Tsiakaras P. CO tolerance and durability study of PtMe (Me= Ir or Pd) electrocatalysts for H2-PEMFC application. Int J Hydrogen Energy 2021;46(26):13865–77.
[43] Pei P, Xu Y, Wang M, Ren P. Effects of carbon monoxide on proton exchange membrane fuel cells and elimination techniques. Int J Hydrogen Energy 2024;69: 1287–304.